Characterization of the RD50-MPW4 HV-CMOS pixel sensor

B. Pilsl[a,*], T. Bergauer[a], R. Casanova[e], H. Handerkas[a], C. Irmler[a], U. Kraemer[c], R. Marco-Hernandez[g], J. Mazorra de Cos[g], F. R. Palomo[f], S. Powell[b], P. Sieberer[a,1], J. Sonneveld[c], H. Steininger[a], E. Vilella[b], B. Wade[b], C. Zhang[b], S. Zhang[d]

[a]*Austrian Academy of Sciences, Institute of High Energy Physics, Nikolsdorfergasse 18, 1050, Vienna, Austria*
[b]*Department of Physics, University of Liverpool, Oliver Lodge Building, Oxford Street, L69 7ZE, Liverpool, UK*
[c]*NIKHEF, Science Park 105, 1098 XG, Amsterdam, Netherlands*
[d]*Physikalisches Institut, Rheinische Friedrich-Wilhelms-Universitaet Bonn, Nussallee 12, 53115, Bonn, Germany*
[e]*Institute for High Energy Physics (IFAE), Autonomous University of Barcelona (UAB), Bellaterra, 08193, Barcelona, Spain*
[f]*Department of Electronic Engineering, University of Sevilla, Calle San Fernando 4, 41092, Sevilla, Spain*
[g]*Instituto de Fisica Corpuscular (IFIC), CSIC-UV, Parque Cientifico, Catedratico Jose Beltran 2, 46980, Paterna (Valencia), Spain*

Abstract

The RD50-MPW4 is the latest HV-CMOS pixel sensor from the CERN-RD50-CMOS working group, designed to evaluate the HV-CMOS technology in terms of spatial resolution, radiation hardness and timing performance. Fabricated by *LFoundry* using a 150nm process, it features an improved architecture to mitigate crosstalk, which has been an issue with the predecessor RD50-MPW3 [1, 2], allowing more sensitive threshold settings and full matrix operation. Enhancements include separated power domains for peripheral and in-pixel digital readout, a new backside-biasing process step, and an improved guard ring structure supporting biasing up to 500 V, significantly boosting radiation hardness. Laboratory measurements and test beam results presented in this paper show significant improvements over its predecessor regarding noise behavior, spatial resolution, and efficiency.

Keywords: RD50-MPW, HV-CMOS, DMAPS, CERN-RD50

1. Characteristics

The RD50-MPW4 comprises a 64×64 pixel matrix with a pitch of $62 \times 62 \mu m^2$. The threshold of each pixel can be tuned by a 4 bit trimDAC. Whilst all sensors are fabricated using a $3\,k\Omega cm$ resistivity substrate, a subset of sensors was backside processed to allow backside biasing and to improve radiation hardness. In this additional process step the sensors were thinned from $300\,\mu m \rightarrow 280\,\mu m$, an additional p^+ layer was implanted and the wafer backside was metallised with titanium and aluminium.

2. Laboratory Assessments

To qualify the trimDACs capabilities to harmonize the pixel response, injection measurements with the in-pixel injection capacitance of $C \approx 2.8\,fF$ (design value) were performed. In this measurement, the threshold voltage was set to a fixed value while the injection voltage was swept on. 100 injections were performed for each injection step, and the digital readout was used to determine the number of detected pulses. The injection voltage $V_{inj,\,50}$ at which 50% of the injected hits get detected was measured in figure 1 and shows a standard deviation of $\sigma \approx 50 e^-$ after adjusting the in-pixel trimming DACs appropriately. Without trimming those for the individual pixels, a width of $\sigma \approx 330\,e^-$ is measured.
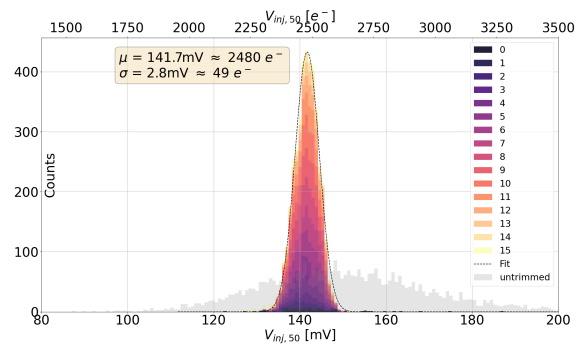

Figure 1: Histogram showing $V_{inj,\,50}$ after harmonizing the pixel response by utilizing the trimDACs. The used trimDAC values are color-coded. The grey histogram in the background shows the pixel response with an equal trimDAC value of 7 for all pixels. The global threshold voltage was set to 950 mV with the baseline being fixed at 900 mV.

---

*Corresponding author
  Email address: Bernhard.Pilsl@oeaw.ac.at (B. Pilsl)
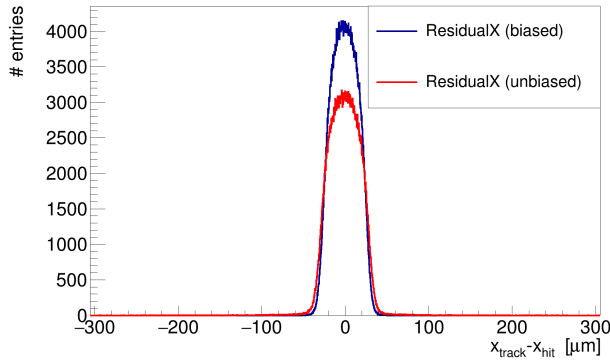[1]Now at Paul Scherrer Institut (PSI).

Figure 2: The unbiased residuals in the X direction show the difference in the extrapolated track's position at the DUT and the detected cluster center. Evaluating the innermost 99 % for the RMS calculation corresponds to the range of $(-43.88\,\mu m, 43.63\,\mu m)$.

Characterisitcs	X-Axis	Y-Axis
RMS (unbiased Residuals)	$16.99\,\mu m$	$17.35\,\mu m$
RMS (biased Residuals)	$14.67\,\mu m$	$13.65\,\mu m$
Geometric mean	$15.79\,\mu m$	$15.39\,\mu m$

Table 1: Spatial resolution characteristics extracted from the analysis of the spatial residuals.

3. Test-Beam Results

To evaluate the sensor's performance in an actual particle beam, a test campaign was conducted at *DESY* [3]. In this campaign, a 4.2 GeV electron beam and the *Adenium* telescope [4] were used. Analysis of the data was done utilizing the *Corryvreckan* [5] framework. The standard parameters for bias voltage and threshold settings for both biasing flavors are $V_{\text{Bias}} = -190\,\text{V}$ and $V_{\text{Thr}} = 30\,\text{mV} \quad \cong \quad Q_{\text{Thr}} \approx 2500\,e^-$.

The spatial residuals, as shown in figure 2, allow to depict the spatial resolution of the sensor. By truncating both distributions to the innermost 99% and calculating the geometric mean of the RMS of the biased and unbiased residuals, the spatial resolution is evaluated as $15.79\,\mu m$ in X and $15.39\,\mu m$ in Y, with the results presented in table 1. The binary resolution of $62\,\mu m/\sqrt{12} \approx 17.9\,\mu m$ is exceeded by taking advantage of the average cluster size of 1.3 pixels per cluster and applying a charge weighted center of gravity calculation for the cluster positions. The minor discrepancy between the two dimensions still must be clarified and is under investigation.

In figure 3 efficiency measurements show full efficiencies $> 99\%$ up to thresholds of $200\,\text{mV}$ which corresponds to $O(5000\,e^-)$. The efficiency drop at higher thresholds is caused by a degraded in-pixel-efficiency at the pixel corners. These effects are more pronounced in the topside-biased samples than the backside-biased ones. The electric field of the backside biasing approach, which is expected to be more uniform, is suspected to be the main cause for the better performance. Further measurements, especially with irradiated samples, are planned to clarify the differences.
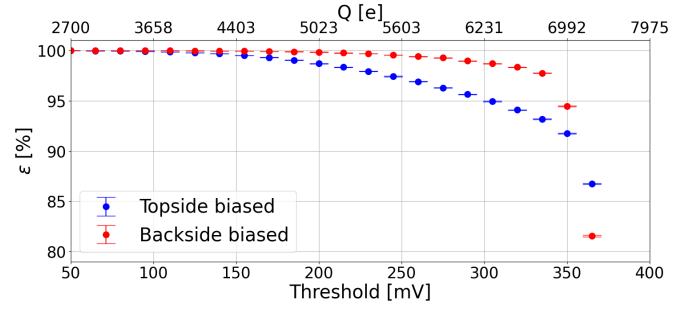

Figure 3: The total efficiency as a function of the applied threshold.

4. Conclusion

Laboratory and test beam measurements have demonstrated that the RD50-MPW4 sensor successfully addressed several issues present in its predecessor. A comparison between the topside and backside biasing schemes reveals that backside biasing is superior, as evidenced by efficiency at high thresholds.

5. Acknowledgements

References

[1] P. Sieberer, et al., Rd50-mpw3: a fully monolithic digital cmos sensor for future tracking detectors, JINST 18 (2023) C02061. doi:10.1088/1748-0221/18/02/C02061.

[2] C. Zhang, et al., Rd50-mpw: a series of monolithic high voltage cmos pixel chips with high granularity and towards high radiation tolerance, JINST 19 (2024) C04059. doi:10.1088/1748-0221/19/04/C04059.

[3] R. Diener, et al., The desy ii test beam facility, NIM - A 922 (2019) 265–286. doi:https://doi.org/10.1016/j.nima.2018.11.133.

[4] L. Yi, et al., Adenium — a demonstrator for a next-generation beam telescope at desy, JINST 18 (2023) P06025. doi:10.1088/1748-0221/18/06/p06025.

[5] D. Dannheim, et al., Corryvreckan: a modular 4d track reconstruction and analysis software for test beam data, JINST 16 P03008 (2021). doi:10.1088/1748-0221/16/03/p03008.